A Compact Penta-Band Printed Monopole Antenna for Multiple Wireless Communication Systems

Sudipta Das, Apurba Chowdhury, Bikram Lala, Ravi Prakash Dwivedi, K. Vasu Babu, and Mohammed EL Ghzaoui

Abstract A compact offset microstrip line-fed printed multiband monopole antenna is proposed. In this work, the suggested antenna operates at multiple resonant frequencies due to the incorporation of narrow parallel slits and a hammer-shaped slot on the radiating patch with a modified ground plane. The proposed antenna has been configured on a 26×25 mm^2 FR-4 substrate ($\varepsilon_r = 4.4$ and thickness $= 1.6$ mm). The simulated return loss results confirm the penta-band resonances from 2.9 to 3.2 GHz, 3.22 to 3.65 GHz, 5.6 to 6.5 GHz, 7.8–8.4 GHz, and 9.4–11.1 GHz to support multi-standard wireless systems such as maritime radio navigation, Wi-MAX, WLAN, X-band satellite communication uplink, ITU band, and aeronautical radio navigation bands. The simulated antenna parameters such as VSWR, radiation pattern, gain and directivity along with surface current distribution have been analyzed in detail and presented in this article. The designed structure maintains VSWR < 2 within the operating penta-bands which indicates very low mismatch losses in the design consideration. Furthermore, almost stable radiation patterns are obtained at all the operating frequencies. Simulated maximum peak gain of about 3.43 dBi at 5.8 GHz is reported for the proposed design.

Keywords Printed antenna · Multiband antenna · Slot · Modified ground plane · Wireless communication

S. Das (✉) · B. Lala
Department of Electronics and Communication Engineering, IMPS College of Engineering and Technology, Malda, West Bengal, India

A. Chowdhury
Mallabhum Institute of Polytechnic, Bishnupur, Bankura, India

R. P. Dwivedi
SENSE, VIT University Chennai Campus, Chennai, Tamilnadu, India

K. Vasu Babu
Department of Electronics and Communication Engineering, Vasireddy Venkatadri Institute of Technology, Guntur, India

M. EL Ghzaoui
Intelligent Systems Networks and Telecommunications Team, IMAGE Laboratory, ENS-Moulay Ismail University of Meknes, Meknes, Morocco

A. Sivasubramanian et al. (eds.), *Futuristic Communication and Network Technologies*, Lecture Notes in Electrical Engineering 792,
https://doi.org/10.1007/978-981-16-4625-6_11

1 Introduction

In the last few years, the expeditious progressive expansion of wireless communication systems necessitates an unbelievable demand of multiband antennas. The lightweight, low-cost and compact microstrip antennas are preferred to be used in modern wireless communication applications. The portability, cost-effectiveness and better performance are the major key concerns for the primary components that are used in wireless devices. As the microstrip antenna is one of the vital components in wireless devices, the design and implementation of miniaturized microstrip antenna [1, 2] is on high demand to make the wireless devices portable. Other than compactness, there is an increasing demand for a single antenna that can support many wireless systems operating at distinct frequency bands. Usually, the employment of many single-band antennas will increase the size and cost of implementation. These requirements lead to the usage of a compact multiband antenna to execute several applications on a single device. Nowadays, researchers have put great efforts to design multiband antennas through different design techniques such as defected microstrip structure [3], fractal [4], and defected ground structure [5]. In addition to these, different monopole configurations have been adopted for achieving multiband functionally, such as loading circular split ring resonator [6], incorporating pair of L-shaped slots [7], using an F-shaped radiator [8], dual-coupled strips of C-shape [9], E- and C-shaped radiators [10], modified patch loaded with multiple strips [11], step-shaped feed line connected with folded slots loaded patch [12], complementary split ring resonator [13], tuning stub[14], meta-material [15], L-loaded IFA [16], modified feed line and parallel strips [17].

The objective of this suggested work is to develop a small multiband antenna with suitable characteristic parameters to support multiple wireless communication systems In this work, a very compact, low profile printed penta-band antenna with an area of 25×26 mm^2 is structured by introducing a slot of hammer shape and three simple parallel slits on the patch along with a modified partial ground plane. The suggested compact antenna radiates at five distinct resonant frequencies with acceptable fractional bandwidth and radiation characteristics to support the multiple numbers of wireless communication applications. The structural design and detailed analysis of the characteristics parameters are performed using MOM-based IE3D software. The proposed antenna offers many advantages such as miniaturized dimension, penta-band operation, low VSWR, good impedance matching and thus low mismatch loss, acceptable gain, directivity, and stable radiation pattern characteristics.

2 Structure of the Proposed Antenna

The geometrical dimensions of the patch can be given as follows [18].

$$W_P = \frac{c}{2f_r}\sqrt{\frac{2}{1+\varepsilon_r}} \tag{1}$$

$$L_P = L_{\text{eff}} - 2\Delta L \tag{2}$$

$$\Delta L = 0.412h \times \frac{(\varepsilon_{\text{re}} + 0.3)\left(\frac{W_p}{h} + 0.264\right)}{(\varepsilon_{\text{re}} - 0.258)\left(\frac{W_p}{h} + 0.8\right)} \tag{3}$$

$$\varepsilon_{\text{re}} = \frac{\varepsilon_r + 1}{2} + \frac{\varepsilon_r - 1}{2}\left[1 + 12\frac{h}{w_p}\right]^{-1/2} \tag{4}$$

$$L_{\text{eff}} = \frac{c}{2f_r\sqrt{\varepsilon_{\text{re}}}} \tag{5}$$

where f_r is the operating frequency of the antenna, W is the width of the radiating patch, L_{eff} is the effective length of the radiator, and ΔL represents the extended normalized lengths of the patch.

The width of the microstrip line is calculated using the following equations [19]

$$\frac{W}{h} = \frac{2}{\pi}\left[B - 1 - \ln(2B-1) + \frac{\varepsilon_r - 1}{2\varepsilon_r}\left\{\ln(B-1) + 0.39 - \frac{0.61}{\varepsilon_r}\right\}\right] \tag{6}$$

where $B = \frac{377\pi}{2Z_0\sqrt{\varepsilon_r}}$.

The length of 50-Ω microstrip line is calculated as

$$L = \frac{\lambda_{\text{ge}}}{2.348} \tag{7}$$

where Effective wavelength (λ_{ge}) is calculated from

$$\lambda_{\text{ge}} = \frac{\lambda}{\sqrt{\varepsilon_{\text{re}}}} \text{ Where, } \varepsilon_{\text{re}} = \text{Effective dielectric constant.} \tag{8}$$

The length of the partial ground plane can be calculated using the following empirical equation:

$$L_g = L_p + 6.25h \tag{9}$$

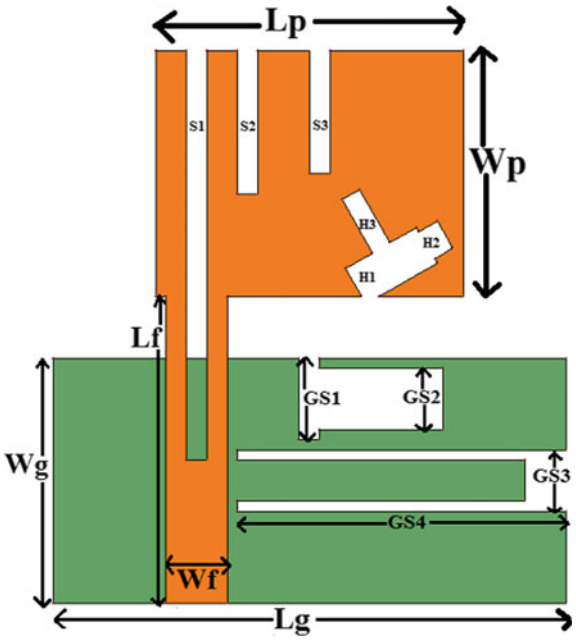

Fig. 1 Layout of the designed multiband monopole antenna

The suggested multiband antenna is shown in Fig. 1. The easily available cost-effective 1.6 mm thick FR-4 substrate with a loss tangent of 0.02 is applied for the design purpose. The designed structure occupies a total area of only 25 × 26 mm^2. The top side of the suggested antenna has been configured by introducing a hammer-shaped slot along with triple parallel slits into the microstrip line fed 15 × 12 mm^2 patch. The back plane of the antenna is comprised of a modified ground structure of 25 × 12mm^2. The optimal structural parameters are summarized as $L_P = 15$ mm, $W_P = 12$ mm, $W_g = 12$ mm, $L_g = 25$ mm,$W_f = 3$ mm, $L_f = 14$ mm, S1 = 20 mm, S2 = 8 mm, S3 = 6 mm, H1 = 4 mm, H2 = 1.5 mm, H3 = 3 mm, GS1 = 4 mm, GS2 = 3 mm, GS3 = 3 mm, GS4 = 14 mm.

3 Structural Development of the Proposed Antenna

The final geometry of the suggested penta-band antenna is constructed after some modifications in the initial design. The structural deployment is depicted in Fig. 2. The desired configuration is obtained after changing the feeding position of the reference antenna and then by introducing various slots on the patch and the ground plane. In case-I, single band performance is observed from 9.286 GHz to 10.403 GHz for − 10 dB S_{11} parameter with a resonant frequency of 9.863 GHz. In case II, the feeding position of the antenna is changed. After changing the feeding position, the same structure as of case I show triple band characteristics. The antenna structure shown

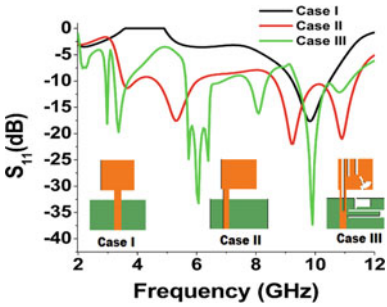

Fig. 2 S_{11} parameters for different stages of structural development

in case II provides −10 dB impedance bandwidths from 3.53 to 3.90 GHz, 4.70 GHz to 6.02 GHz, and 8.698 GHz to 11.4 GHz. But the intended applications such as WiMAX (3.3–3.6 GHz), X-band satellite communication uplink (7.9–8.4 GHz), and ITU (8–8.4 GHz) bands are not covered in the design case II. In the final design step (case III), the structure has been modified through slot perturbations on the patch as well as the ground plane. The suggested modifications in case III lead to achieving penta-band operation and the antenna structure covers frequency bands of 30 MHz (2.9–3.2 GHz), 430 MHz (3.22–3.65 GHz), 900 MHz (5.6–6.5 GHz), 600 MHz (7.8–8.4 GHz), and 1700 MHz (9.4–11.1 GHz). Hence, the layout (Case III) shown in Fig. 2 is considered as the proposed antenna configuration for the intended wireless applications such as maritime radio navigation (3 GHz), Wi-MAX (3.3–3.6 GHz), WLAN (5.725–5.825 GHz), X-band satellite communication uplink (7.9–8.4 GHz), ITU band (8–8.4 GHz), and aeronautical radio navigation (10–10.7 GHz) bands.

4 Explanation of the Surface Current Distribution

The variations of the surface current in the proposed penta-band antenna are presented in this section. Surface current distributions at different operating frequencies (3.05, 3.435, 6.05, 8.1, and 10.25 GHz) are investigated and displayed in Figs. 3a–e). An explanation of the variations in surface current distribution on the designed antenna for different operating frequencies will add some key insights regarding the structural validation of the proposed configuration and its excitation behavior to understand the working of the suggested antenna. For the 3.05 GHz operation, it can be observed from Fig. 3a that the surface currents strongly circulate around the vertically placed parallel slits and the vertical arm of the hammer-shaped slot which controls the resonance excitation of the first operating band (2.9–3.2 GHz). However, the second operating band is mainly generated and controlled by the slots incorporated in the partial ground plane as shown in Fig. 3b for 3.435 GHz. As observed from Fig. 3c, the center frequency (6.05 GHz) of the third resonance band is dependent on the slots loaded on both the patch and ground plane. A very dense surface current is noticed around the hammer-shaped slot along with the shortest vertical slit loaded

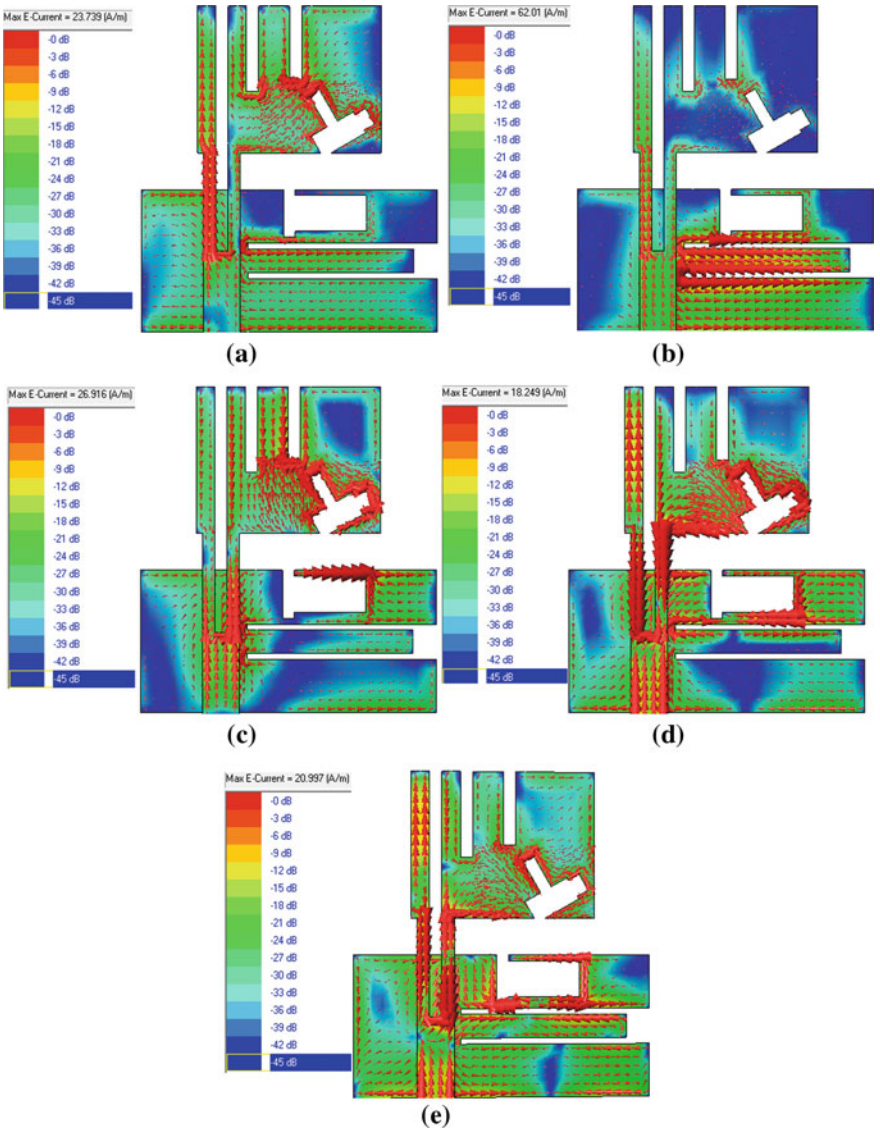

Fig. 3 Presentation of surface current variations at **a** 3.05 GHz, **b** 3.435 GHz, **c** 6.05 GHz, **d** 8.1 GHz, and **e** 10.25 GHz

on the patch and the horizontal arm of the open-ended slot in the ground plane. For the fourth resonance band with center frequency 8.1 GHz, the originated surface currents strongly circulate around the longest vertical slit and hammer-shaped slot on the patch along with a wide open-ended slot in the partial ground plane [see Fig. 3d]. Finally, for 10.25 GHz, it is observed from Fig. 3e that the maximum

surface current is distributed along the defected ground plane structure, longest slit incorporated on the patch, and vertical arm of the hammer-shaped slot for which the fifth operating band is generated. The comprehensive analysis of the surface current distribution helps to understand the working mechanism of the designed antenna. The incorporated slots on the patch and ground plane have changed the electric and magnetic field distributions which further varies the mean current path of any resonant mode and as a result number of resonant frequency increases. Furthermore, the shifting of resonant frequencies to lower values may be explained by the fact that the concentration of the surface currents is enhanced around the sides of the slots and the elongation of the distributed surface current increases the current path thus making the antenna electrically larger thereby the excited resonant frequency decreases.

5 Results and Discussion

The simulation results of the presented antenna in terms of S_{11} parameter and VSWR are shown in Fig. 4. A clear observation shows that the suggested structure resonates at penta-band for VSWR < 2 and $S_{11} < -10$ dB. The results depicts five distinct frequency bands with impedance bandwidths (IBW) of 30 MHz (2.9–3.2 GHz, fractional bandwidth = 9.836%), 430 MHz (3.22–3.65 GHz, fractional bandwidth = 12.518%), 900 MHz (5.6–6.5 GHz, fractional bandwidth = 14.876%), 600 MHz (7.8–8.4 GHz, fractional bandwidth = 7.407%), and 1700 MHz (9.4–11.1 GHz, fractional bandwidth = 16.583%). The VSWR lies within 2:1 signifies good impedance matching and acceptable mismatch loss across the penta-band of operation. The variations of gain and directivity for the designed penta-band antenna are depicted in Fig. 5. A peak gain of about 3.46dBi is obtained at 5.8 GHz while the directivity reaches to a maximum value of 6.15dBi at 10.40 GHz. Figure 6a, b presents the radiation patterns of the designed penta-band antenna. The E and H plane radiation patterns are described for the center operating frequencies of each band, 3.05, 3.435, 6.05, 8.1, and 10.25 GHz, respectively. The proposed antenna offers almost stable monopole-like radiation responses at both the planes (E and H) but slight deterioration

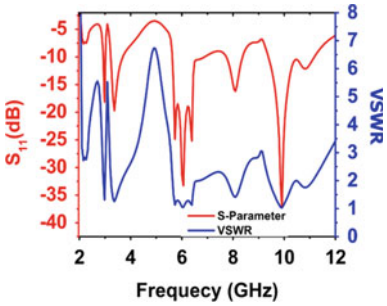

Fig. 4 S_{11} and VSWR of the proposed antenna

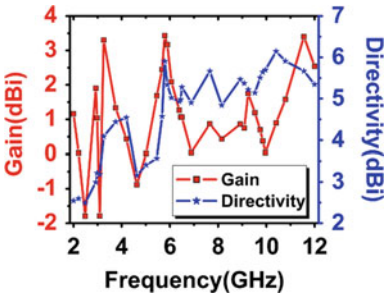

Fig. 5 Gain and Directivity versus frequency

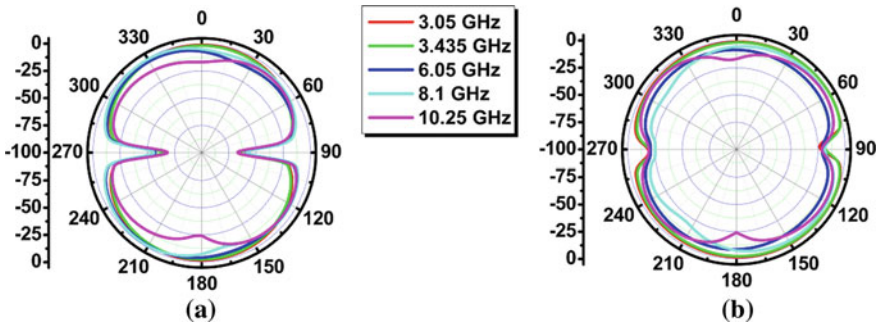

Fig. 6 Radiation pattern characteristics **a** E-plane **b** H-plane

is noted with an increase in frequency mainly at 10.25 GHz. The maximum radiation intensity is observed towards 0° with linear polarization. The E-plane patterns almost resemble a figure of "8" while the H-plane patterns resemble an oval-shaped with slight distortions at the upper band frequency.

6 Conclusion

A small printed antenna has been proposed in this article for maritime radio navigation, Wi-MAX, WLAN, X-band satellite communication uplink, ITU band, and aeronautical radio navigation bands. The presented antenna is suitable for penta-band operation. The proposed antenna has been configured by incorporating a hammer-shaped slot and vertical slits of different lengths on the patch and reformed ground plane. The presented radiator resonates at five distinct frequency bands at about 3.05, 3.435, 6.05, 8.1, and 10.25 GHz with desired stable radiation patterns and acceptable gains. Also, good impedance matching and thus low mismatch losses are obtained across the operating frequency bands. So, the proposed antenna is compact, low profile, easy to realize, offers penta-band operation and supports several wireless applications.

References

1. Das S, Sarkar PP, Chowdhury SK (2014) Design and analysis of a compact monitor-shaped multifrequency microstrip patch antenna. J Electromagn Waves Appl 28(7):827–837
2. Das S, Sarkar PP, Chowdhury SK (2015) Modified π-shaped slot loaded multifrequency microstrip antenna. Progress Electromagn Res B 64(1):103–117
3. Salamin MA, Das S, Zugari A (2018) Design and realization of low profile dual-wideband monopole antenna incorporating a novel ohm (Ω) shaped DMS and semi-circular DGS for wireless applications. AEU-Int J Electron Commun 97:45–53
4. Ali T, Aw MS, Biradar RC (2018) A fractal quad-band antenna loaded with L-shaped slot and metamaterial for wireless applications. Int J Microw Wirel Technol 10:826–834
5. Kunwar A, Gautam AK, Kanaujia BK (2017) Inverted L-slot triple-band antenna with defected ground structure for WLAN and WiMAX applications. Int J Microw Wirel Technol 9:191–196
6. Baba MA, Rahim MKA, Zubir F, Fairus M, Yusoff M (2018) Design of miniaturized multiband patch antenna using CSRR for WLAN/WiMAX applications. Telkomnika 16(4):1838–1845
7. Chen S, Fang M, Dong D, Han M, Liu G (2015) Compact multiband antenna for GPS/WiMAX/WLAN applications. Micowave Opt Technol Lett 57(8):1769–1773
8. Ren W, Hu SW, Jiang C (2017) An ACS-fed F-shaped monopole antenna for GPS/WLAN/WiMAX applications. Int J Microw Wirel Technol 9:1123–1129
9. Han Y, Yin YZ, Wei YQ, Zhao Y, Li B, Li XN (2011) A novel triple-band monopole antenna with double coupled c-shaped strips for wlan/wimax applications. J Electromagn Waves Appl 25:1308–1316
10. Honarvar MA, Hamidi N, Virdee BS (2015) Multiband antenna for portable device applications. Microw Opt Technol Lett 57:956–959
11. Mondal K, Samanta A, Sarkar PP (2017) Compact multiband monopole antenna for ISMband 2.4 GHz, Bluetooth, WiMAX Wi-Fi applications. Wirel Pers Commun 97:181–195
12. Jalali AR, Ahamdi JS, Emadian SR (2016) Compact multiband monopole antenna for UMTS, WiMAX, and WLAN applications. Microw Opt Technol Lett 58:844–847
13. Daniel RS, Pandeeswari R, Raghavan S (2017) Multiband monopole antenna loaded with-complementary split ring resonator and C-shaped slots. AEU-Int J Electron Commun 75:8–14
14. Brar RS, Saurav K, Sarkar D, Srivastava KV (2018) A quad-band dual-polarized monopole antenna for GNSS/UMTS/WLAN/WiMAX applications. Microw Opt Technol Lett 60:538–545
15. Ali T, Khaleeq MM, Pathan S, Biradar RC (2017) A multiband antenna loaded with metamaterial and slots for GPS/WLAN/WiMAX applications. Microw Opt Technol Lett 60:79–85
16. Al-Khaldi M (2017) A highly compact multiband antenna for Bluetooth/WLAN, W-MAX, and Wi-Fi Applications. Microw Opt Technol Lett 59:77–80
17. Bag B, Biswas P, Sarkar S, Sakar PP, Ghosal D (2020) Novel monopole microstrip antennas for GPS, WiMAX and WLAN applications. J Circuits Syst Comput 29(3):2050050
18. Balanis CA (2005) Antenna theory analysis and design, 3rd edn. Hoboken, NJ, USA, Wiley
19. David M (2005) Pozar: microwave engineering, 3rd edn. Wiley, USA